



## Generation of Nanostructured MgO Particles by Solution Phase Method

Chandruppa K.G.<sup>1\*</sup>, Venkatesha T.V.<sup>2</sup>, Praveen B.M.<sup>3</sup> and Shylesha B.S.<sup>4</sup>

<sup>1</sup>Department of Chemistry, Government Engineering College, B.M. Road, Ramanagara, INDIA

<sup>2</sup>Department of P.G. Studies and Research in Chemistry, Kuvempu University, Shankaraghatta, INDIA

<sup>3</sup>Department of Chemistry, Srinivas School of Engineering, Mukka, Mangalore, INDIA

<sup>4</sup>Department of Chemistry, Sri Siddaganga College of Arts, Science and Commerce, Tumkur, INDIA

Available online at: [www.isca.in](http://www.isca.in), [www.isca.me](http://www.isca.me)

Received 16<sup>th</sup> March 2015, revised 15<sup>th</sup> April 2015, accepted 9<sup>th</sup> May 2015

### Abstract

*In this contribution, disc like nanosized MgO particles were successfully synthesized by solution-phase method using magnesium chloride (MgCl<sub>2</sub>) and sodium hydroxide (NaOH) in ethanol medium. The ethanol and water content were varied and the generated precursor compound was calcined for an hour at temperature of 300 °C. Samples were characterized by XRD, SEM, FT-IR and UV-Vis spectroscopic techniques. The crystallite sizes were in the range of 17–35 nm based on Debye-Scherrer equation. Scanning electron photomicrographs suggest that all the samples were well crystalline, randomly oriented disc like morphology. The FT-IR result shows strengthen other results and also blue shift was noticed in UV-Vis absorption spectra.*

**Keywords:** Solution phase, Nanoparticle, X-ray diffraction, MgO, Ethanol.

### Introduction

In the last decade, a great deal of attention has been focused on nanosized materials because of their unusual physical, chemical and mechanical properties<sup>1,2</sup>. The difference in chemical properties in particular, as compared to bulk material the nanomaterials are almost large surface area and a great increase in number of active sites on the surface such as corners, edges and dislocations. Furthermore, the nanomaterials are usually less thermodynamically stable than corresponding bulk materials which contributes to their enhanced chemical activity<sup>1</sup>. Oxide nanomaterials are finding a wide range of applications as catalysts and starting materials for preparing advanced structural ceramics because they possess a unique property, i.e., high reactivity, resulting from their high specific surface area, controlled size and distribution. Among those properties oxides, magnesium oxide is more attractive for both fundamental and applicable research areas. Nanocrystals of common metal oxides such as MgO, CaO and ZnO have been shown to be highly efficient and active adsorbents for many toxic chemicals including air pollutants, chemical warfare agents and acidic gases. In particular, the adsorptive properties of MgO are diverse and many works have been reported on the adsorption of H<sub>2</sub>, CO, H<sub>2</sub>O, NH<sub>3</sub>, Pyridine etc<sup>1,3</sup>. Nanosized particles of TiO<sub>2</sub>, Al<sub>2</sub>O<sub>3</sub>, ZnO and MgO are a group of metal oxides that possess photocatalytic ability, electrical conductivity, UV absorption and photo-oxidizing capacity against chemical and biological species<sup>4</sup>. Although, many metal oxides such as MgO, CaO, TiO<sub>2</sub>, ZrO<sub>2</sub>, FeO, V<sub>2</sub>O<sub>3</sub>, V<sub>2</sub>O<sub>5</sub>, Mn<sub>2</sub>O<sub>3</sub>, Fe<sub>2</sub>O<sub>3</sub>, NiO, CuO, Al<sub>2</sub>O<sub>3</sub>, ZnO and their mixtures may be capable of such surface chemistry, MgO serves as a good sculpt since it possesses a simple crystal structure and because it can be prepared by different methods with wide range of surface area. Additionally, MgO has exhibited high reactivity in catalytic processes and its

defect sites have been shown to be active sites<sup>5,6</sup>. The high surface reactivity, high chemical and thermal stability makes this MgO as a promising material for different applications like sensors, catalysis, paints, additives, etc<sup>7</sup>. Nanosized MgO is a functional material that has been widely used in various areas and recently it has been reported that MgO has a good bactericidal performance in aqueous environments<sup>8,9</sup>. The two pioneers in this area are Klabunde et al.<sup>10</sup> and Aharon et al.<sup>11</sup>, who demonstrated that nano-MgO exhibits high activity against bacteria, spores and viruses because of its large surface area. Magnesium oxide is also used in variety of industrial applications in high-temperature insulating materials, heat-resistant glass composite in liquid crystal display panels, electroluminescence display panels, plasma display panels, heat-resistances, fuel-oil additives and fluorescent display tubes<sup>12-14</sup>. A composite fiber with nanoparticle of TiO<sub>2</sub>/MgO can provide self-sterilizing function<sup>4</sup>. Thin films of MgO are also of interest in areas such as insulators for magnetic tunnel junctions<sup>15,16</sup> or high-k dielectrics (bandgap 7.8 eV)<sup>17,18</sup>. Magnesium oxide (periclase) crystallizes in cubic symmetry (NaCl structure); platelike particles are uncommon for MgO<sup>19</sup>.

There are several methods for preparing MgO including high-temperature solid state synthesis, vapor-phase oxidation<sup>20</sup>, sol-gel techniques<sup>21</sup>, precipitation<sup>22</sup>, conventional spray pyrolysis<sup>23</sup>, thermal decomposition<sup>19</sup>, chemical solution deposition<sup>24</sup>, coprecipitation<sup>25</sup>, combustion<sup>26</sup>, plasma enhanced chemical vapour deposition, molecular beam epitaxy and sputtering method have been frequently employed. All these methods require high temperature and expensive instruments<sup>7</sup>. The oxide morphology and particle sizes are dependent on such preparation conditions as the pH, temperature of precipitation, concentration or ionic strength, and calcination temperature/time<sup>27</sup>. Therefore, research continues into achieving better control over the sizes of MgO

particles through smart chemical processing of materials.

Nowadays, the solution-phase approach has become a promising technique to prepare nanostructures<sup>28</sup>. During the solution-phase synthesis of nanoparticles, the control of nucleation and successive growth, which is extremely sensitive to the synthetic parameters, has been believed to be the key to the size- and shape-controlled synthesis of nanostructures<sup>29,30</sup>. Solution-phase processing affords nanoparticles and nanocomposites of a wide range of materials, including metals, alloys, intermetallics and ceramics, with substantial control of particle size, particle morphology, microstructure and composite microstructure<sup>31</sup>. Longshan Xu<sup>32</sup>, have prepared single-crystal hollow cuprous oxide (Cu<sub>2</sub>O) spheres with nanoholes using glucose as the reducing agent and gelatin as a soft template. Dongning Yang<sup>33</sup> synthesized magnesium hydroxide sulfate hydrate nanoribbons by solution-phase approach. Louis A. Carpino<sup>34</sup>, prepared rapid continuous solution synthesis of peptide segments. Bryan D. Wood<sup>35</sup>, synthesized crystalline lithium niobate nanoparticles of uniform dimensions, shape and composition by solution phase method.

More recently, we have explored a relatively new simple technique for well optimized synthesis of MgO nanoparticle by solution phase method. Since the low-temperature approaches have the advantages of relatively low cost, high purity and potential for scaling up, exploring these methods appears quite important. The Scanning electron microscopic (SEM) images and X-ray diffraction (XRD) technique were taken to characterize the MgO nanoparticles. The Fourier transform infrared spectra (FT-IR) and UV-Visible absorption techniques of these samples were documented.

## Material and Methods

**Starting materials and synthesis of MgO nanoparticles:** In a typical synthesis, 203.3 mg (20 mM) of MgCl<sub>2</sub> were dissolved in 50 ml of ethanol (Solution A). Second, 80 mg (40 mM) of NaOH were dissolved in 50 ml of Ethanol (Solution B). Both the solution was kept in a separate Magnetic stirrer at 60 °C, for 30 min. Under intense stirring, the solution B was added dropwise in to solution A by maintaining the temperature at 60 °C. The solution was kept under stirring for 10 min and diluting the solution by adding 20 ml of Ethanol with constant stirring. The precursor solution was then centrifuged at 2000 rpm for 10 min and the obtained residue was dried at 60°C in a hot air oven. The obtained as-prepared compound was calcined at 300 °C for 1 hr to get crystalline MgO nanoparticles. The samples of MgO nanoparticle was also prepared by varying the solvents like ethanol and water ratio, where the concentration of the MgCl<sub>2</sub> and NaOH is remained as the same. The following reaction conditions are shown below.

**Reaction:**  $C_2H_5OH + MgCl_2 + 2NaOH \rightarrow Mg(OH)_2 + 2NaCl$

**Calcination:**  $Mg(OH)_2 \rightarrow MgO + H_2O, 300^\circ C$

**Structural characterization:** Powder X-ray diffraction (XRD)

patterns was recorded for all the samples using XPERT Pro powder diffraction from Philips pan analytical with Cu-K $\alpha$  radiation, ( $\lambda_{Cu}=1.5418 \text{ \AA}$ ) at a scanning rate of 2° / minute with a 0.02° step size in the 2 $\theta$  range 10 - 100° working at 30 mA and 40 kV. Fourier transform infrared spectra (FT-IR) were obtained on KBr pellets at ambient temperature using a Bruker FT-IR spectrometer (SENSOR 27). The morphology of sample was examined by using (Philips XL 30) scanning electron microscopy (SEM). The UV-Visible spectra of MgO nanoparticles dispersed in water were recorded by Elico SL 159 UV-Vis Spectrophotometer. The sample was sonicated prior to UV-Visible spectral measurement, for uniform dispersion.

## Results and Discussion

**Powder X-ray diffraction analysis:** Powder X-ray diffraction pattern in figure-1, indicates that the Monophasic FCC MgO phase is obtained by annealing precursor at 300 °C for all the samples. XRD results are matches with joint committee of powder diffraction standard (JCPDS). The crystal planes of MgO with cubic phase are comparable with standard JCPDS file. XRD confirmed that on calcination at 300°C Mg (OH)<sub>2</sub> was completely converted to nanosized MgO having a face centered cubic phase. The crystallite sizes of prepared samples were calculated from full width at half maxima (FWHM) of all peaks using the Debye Scherer equation. The contraction of lattice parameter with decrease of the crystalline size suggests that surface tension probably plays a major role in determining the lattice parameter. The surface free energy of nanocrystal arises from the surface chemical bonds created during formation. The total surface energy is the product of the number of surface chemical bonds and the surface bond energy<sup>36</sup>. The surface energy increase of nanoparticles will tend to contract their sizes by distorting their crystal lattice elastically. Of course this kind of distortion is very small compared to the whole particle size. Hence particle size decreased due to the concentration of ethanol which is varied with water.

**Scanning Electron Microscopic analysis:** The SEM images of MgO nanoparticles obtained from different volume ratios of ethanol and water by solution phase method and are shown in figure 2. From figure 2(a) and (b) reveals the SEM images of MgO nanoparticles obtained at ethanol: water (30:20) ratio, and we observed that the particles are well defined agglomerated triangular shape and some of them are hexagonal in shape. The size range of particle is almost 17 – 35 nm and is almost agglomerated in triangular shape. Figure 2(c) and (d) shows the SEM photomicrographs of MgO nanoparticles obtained from volume ratio of ethanol:water (45:5) and calcined at 300 °C. The particles become well crystallized, randomly oriented disc like shape. The shapes are oriented disc like structure and the size of the particle increases with ethanol content. The particles are well crystalline and the size is around 25 nm. It can be observed that MgO nanoparticles are mainly present granules with triangular, hexagonal and oriented disc like shaped nanoparticles and are well crystallized in nature.

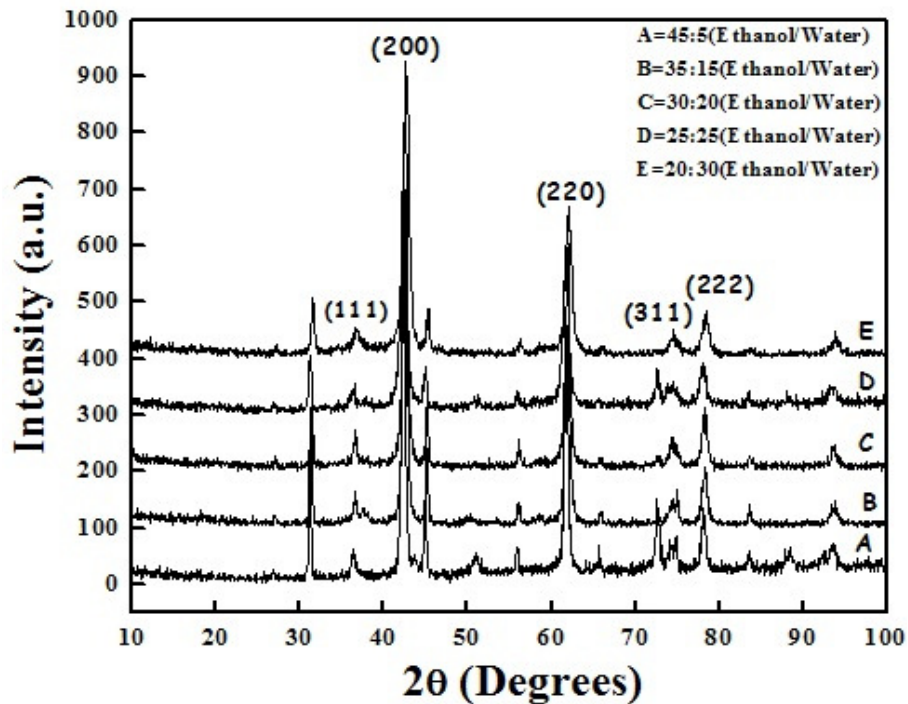


Figure-1  
XRD patterns of MgO obtained from solution-phase and calcined at 300 °C for 1 hr.

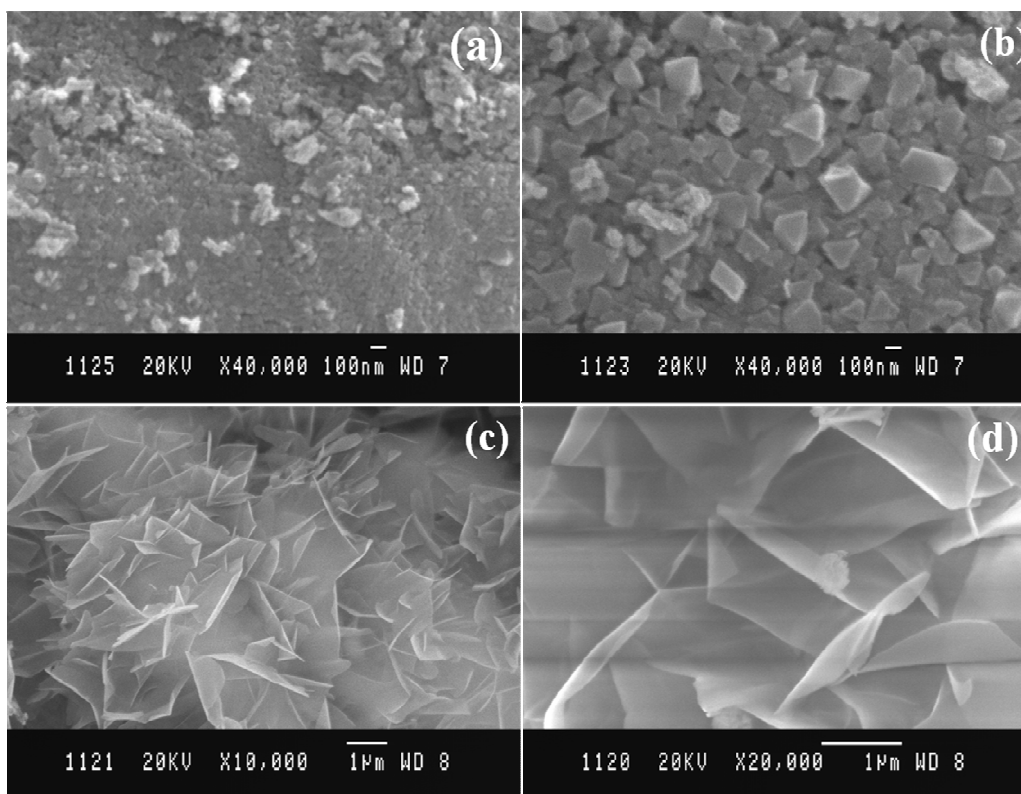


Figure-2  
Scanning electron photomicrographs of MgO nanoparticles (a) as-prepared (b) calcined at 300°C (c) and (d) calcined at 300°C with different magnification (Ethanol: Water ratio 45:5)

**FT-IR spectroscopic studies:** Fourier transform infrared spectroscopy was used to detect the presence of functional groups adsorbed on the surface of synthesized particles during solution phase process. Figure 3 shows the FT-IR spectra of MgO powder obtained from solution phase method and calcined at 300 °C for 1 hr. It indicates that, the strong absorption peak in the range of 3200–3600  $\text{cm}^{-1}$  was observed. This was centered at 3433  $\text{cm}^{-1}$  corresponds to the stretching vibration of intermolecular hydrogen bond (O–H) existing between the adsorbed water molecules and indicates the lower amount of hydroxyl group<sup>37</sup>. The peaks at 1485 and 1625  $\text{cm}^{-1}$  are attached to bending vibrations of  $\text{Mg}(\text{OH})_2$ . The strong band at 456  $\text{cm}^{-1}$  and weak band 865  $\text{cm}^{-1}$  appearing in IR spectrum of calcined (300 °C) compound indicates the presence of stretching and bending vibrations of the intercalated M–O species. The bands below 1000  $\text{cm}^{-1}$  are related to Mg–O absorption<sup>37</sup>. This indicates the presence of MgO nanoparticles in calcined compounds.

**UV-Visible spectroscopic studies:** The UV-Vis spectra of MgO nanoparticles obtained from 20 mM of  $\text{MgCl}_2$  and 40 mM of NaOH in ethanol medium by solution phase route and calcined at 300°C for 1 hr were shown in figure-4. For recording UV-Vis spectra, the sample of MgO solution was prepared by ultrasonically dispersing them in absolute ethanol. The absorption peak in figure 4 correspond to MgO sample

calcined at a temperature of 300°C showing the strong absorption in the wavelength in the range of 321.2 nm. The peak observed in MgO Nanoparticle is due to size distribution of the particles. This can be assigned to the intrinsic band gap absorption of MgO due to the electron transitions from the valence band to the conduction band. The band gap ( $E_g$ ) of MgO nanoparticles was calculated by using the formula  $E_g = hc/\lambda$ , where  $h$  = Planck's constant,  $c$  = velocity of light and  $\lambda$  = wavelength. The corresponding band gap was found to be 6.17 eV. Further, the XRD and SEM results suggest that the MgO particles are in the range of 17–35 nm. It is known that the optical absorption would be affected considerably by the morphology and crystallinity of MgO crystals. The present solution phase method for generating MgO nanoparticles is in the blue region compared to the bulk MgO (7.8 eV).

### Conclusion

The nanosized MgO particles were successfully generated by solution phase method. Prepared MgO nanoparticles were well crystalline and it was confirmed by XRD pattern. The SEM images confirm the samples are present as granules with triangular, hexagonal and oriented disc like shaped particles with 17-35 nm size. It is a simple, eco-friendly and more efficient method for generating MgO nanoparticles.

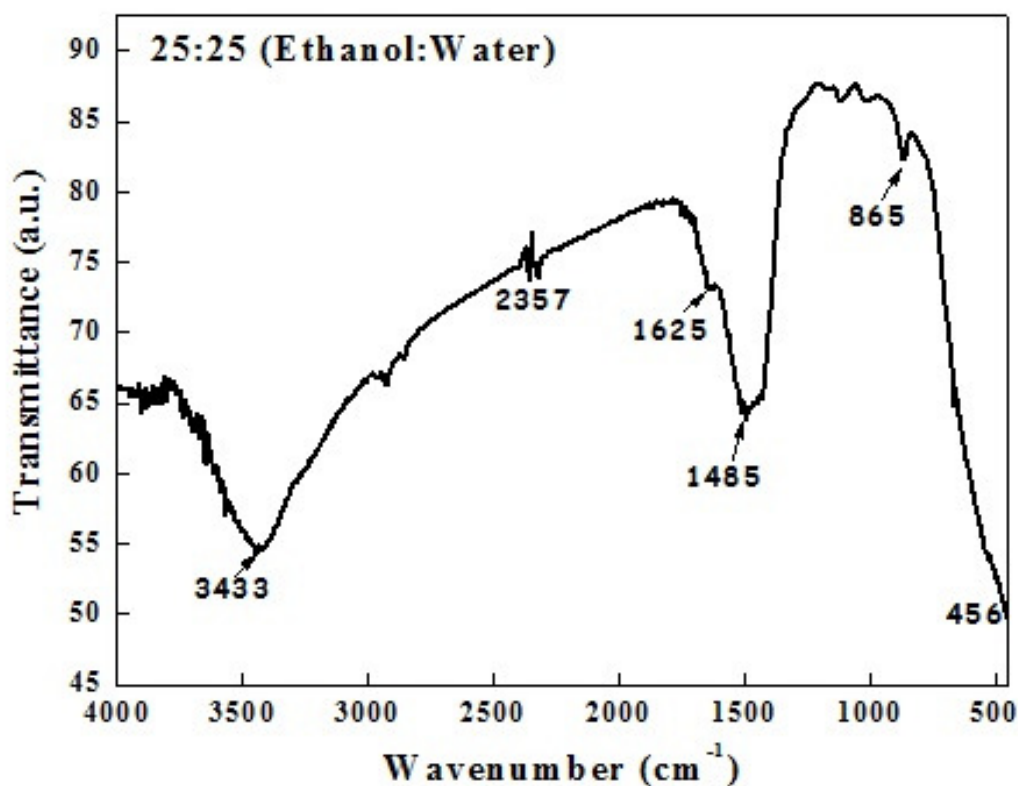


Figure-3  
FT-IR spectra of MgO obtained from 25:25 ethanol: water ratio and calcined at 300 °C for 1hr

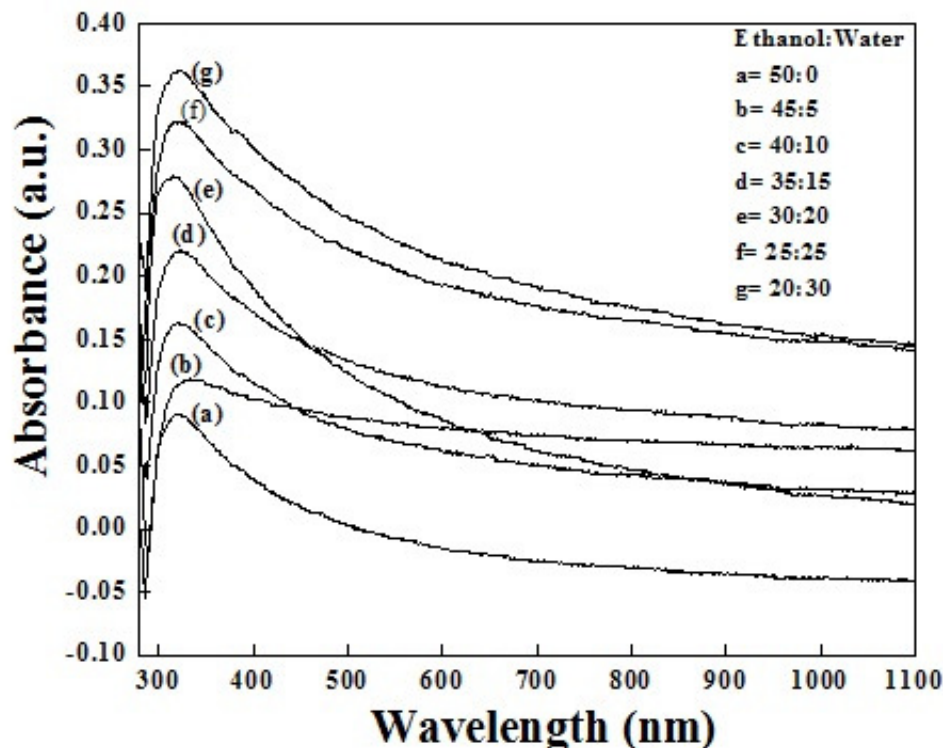


Figure-4

UV-Vis spectra of MgO nanoparticles obtained from different volume ratios of ethanol and water medium

### Acknowledgement

The authors thank to Kuvempu University, Shimoga, and also the first author thank to Department of Technical Education (DTE), Government of Karnataka, Bangalore, Karnataka, India for providing the lab facilities to bring about this work.

### References

1. Kenneth J., Klabunde and Peter K. Stoimenov., Dekker encyclopedia of Nanoscience and Nanotechnology, VI Volume, CRC Press, (2004)
2. Elaheh Esmaeili., Abasali Khadadi and Yadollah mortazavi., Structure and microstructure of combustion synthesised MgO Nanoparticle synthesis using polyethylene glycol and sorbitol, *J. of European ceramic society*, **29**, 1061-1068 (2009)
3. Yong Cheol Hong and Han Sup Uhm, Synthesis of nanopowder in atmospheric microwave plasma torch, *Chem. Phy. Letters*, **422**, 174-178 (2006)
4. Cover story, Nanomaterials, A Big Market Potential, Chemical Week, October **16**, pi 7, (2002)
5. Li Y. and Klabunde K.J., *Langmuir*, **7**, 1388, (1991)
6. Koper O., Klabunde K.J., US. Patent No. 6057488, (2000)
7. Rizwan wahab., Ansari S.G., Dar M.A., Kim Y.S. and Shin H.S., Synthesis of MgO nanoparticles by sol-gel process, *Materi.sci. forum*, **558-559**, 983-986 (2007)
8. Cui Z., Meng G.W., Haung W. D., Wang G.Z. and L. D. Zhang, *Mater. Res. Bull*, **35**, 1653 (2000)
9. Kim H.W., Shim S.H. and Chongmu L., *J. of Korean Phys. Soc*, **49(2)**, 628 (2006)
10. Peter K.S., Rosalyn L., George L.M. and Klabunde J.K., *Langmuir*, **18**, 6679 (2002)
11. MakhluF S., Rachel D., Yeshayahu N., Yaniv A., Raz J. and Aharon G., *Adv. Func. Mater*, **15**, 1708 (2005)
12. Poullikkas A., *Energy Conversion Manage*, **45**, 1725 (2004)
13. Guo X. L., Liu Z. G., Chen X. Y., Zhu S. N., Xiong S. B., Hu W. S. and Lin C. Y., *J. Appl. Phys*, **29**, 1632 (1996).
14. Li Y.R., Liang Z., Zhang Y., Zhu J., Jiang S.W. and Wei X. H., *Thin Solid Films*, **489**, 245 (2005)
15. Parkin S.P.P., Kaiser C., Panchula A., Rice P.M., Hughes B., Samant M. and Yang S.H., *Nat. Mater*, **3**, 862-867 (2004)
16. Yuasa S., Nagahama T., Fukushima A., Suzuki Y. and Ando K., *Nat. Mater*, **3**, 868-871 (2004)

17. Yan L., Lopez C.M., Shrestha R. P., Irene E. A., Suvorova A. A. and Saunders M., *Appl. Phys. Lett*, **88**, 142901 (2006)
18. Posadas A., Walker F.J., Ahn C.H., Goodrich T.L., Cai Z. and Ziemer K.S., *Appl. Phys. Lett*, **92**, 233511 (2008)
19. Fedorov P.P., Tkachenko E.A., Kuznetsov S.V., Voronov V.V. and Lavrishchev S.V., Preparation of MgO Nanoparticles, *Neorganicheskie Materialy*, **43(5)**, 574–576 (2007)
20. Itatani K., Yasuda R., Howell F.S. and Kishioka A., *J Mater Sci.*, **32**, 2977 (1997)
21. Lopez T., Garcia-Cruz I. and Gomez R., Synthesis of Magnesium Oxide by the Sol-Gel Method: Effect of the pH on the Surface Hydroxylation, *Journal of catalysis*, **127**, 75-85 (1991)
22. Baranova A.N., Kapitanova O.O., Panin G.N. and Kang T.V., ZnO/MgO Nanocomposites Generated from Alcoholic Solutions, *Russian Journal of Inorganic Chemistry*, **53(9)**, 1366-1370 (2008)
23. Dae Jong Seo, Seung Bin Park, Yun Chan Kang and Kwang Leong Choy, Formation of ZnO, MgO and NiO nanoparticles from aqueous droplets in flame reactor, *Journal of Nanoparticle Research*, **5**, 199–210 (2003)
24. Mikhail Pashchanka, Rudolf C. Hoffmann and Jhorg J., Schneider, Controlled synthesis and characterisation of MgO nanoparticles, thin films and polycrystalline nanorods derived from an Mg (II) single source precursor, *Journal of Materials Chemistry*, (2009)
25. Zhanlai Ding, Cunran An, Qiang Li, Zhezhe Hou, Jianqiang Wang, Haibo Qi and Fangjuan Qi, Preparation of ITO Nanoparticles by Liquid Phase by Coprecipitation Method, *Journal of Nanomaterials*, (2010)
26. Singanahally T. Aruna, Alexander S. and Mukasyan, Combustion synthesis and nanomaterials, *Current Opinion in Solid State and Materials Science*, **12**, 44-50 (2008)
27. Hur J. M., Kim I. S., Lee W. K., Cho S. H., Seo C. S. and Park S.W., *J. Ind. Eng. Chem*, **10**, 442 (2004), Kim K. D., Kim S.S. and Kim H.T., *J. Ind. Eng. Chem*, **11**, 584 (2005)
28. Xia Y.N., Rogers J.A. and Paul K.E. et al., Unconventional methods for fabricating and patterning nanostructures, *Chem Rev*, **99**, 1823-1848 (1999).
29. Ahmadi T.S., Wang Z.L. and Green T.C. et al., Shape-controlled synthesis of colloidal platinum nanoparticles. *Science*, **272**, 1924-1926 (1996)
30. Nikoobakht B. and El-Sayed M.A., Preparation and growth mechanism of gold nanorods (NRs) using seed-mediated growth method, *Chem Mater*, **15**, 1957-1962 (2003)
31. Joel A. Haber, Nilesh V. Gunda and William E. Buhro, Nanostructure by design: Solution-phase-processing routes to nanocrystalline metals, ceramics, intermetallics and composites, *journal of Aerosol sci*, **29(5-6)**, 637-645 (1998)
32. Longshan Xu, Xiaohua Chen, Yurong Wu and Chuansheng Chen, Solution-phase synthesis of single-crystal hollow Cu Ospheres with nanoholes, *Nanotechnology*, **17**, 1501–1505 (2006)
33. Dongning Yang, JinZhang, Rongming Wang and Zhongfan Liu, Solution phase synthesis of magnesium hydroxide sulfate hydrate nanoribbons, *Nanotechnology*, **15**, 1625–1627 (2004)
34. Louis A. Carpino, Shahnaz Ghassemi, Dumitru Ionescu and Mohamed Ismail, Dean Sadat-Aalae, Rapid, Continuous Solution-Phase Peptide Synthesis: Application to Peptides of Pharmaceutical Interest, *Organic Process Research and Development*, **7**, 28–37 (2003)
35. Bryan D. Wood, Valentin Mocanu and Byron D. Gates, Solution-Phase Synthesis of Crystalline Lithium Niobate Nanostructures, *Adv. Mater*, **20**, 4552–4556 (2008)
36. Ragone D.V., Themodynamics of materials, Vol II. Jhone Wiley and sons Inc. (1995)
37. Haxia Niu, Qing Yang, Kaibian Tang and Yi Xie, Large scale synthesis of single crystalline MgO with bone like nanostructures, *J. of Nanoparticle research*, **8**, 881-888 (2006)